Pūhau ana te rā: Tailwinds

Vol. 2 No. 2 (2024): Pūhau ana te rā 2024

Title: **Carbon Loss from Earthquake-Induced Landslides in Fiordland**

Authors: Charles A. Cox

DOI: 10.11157/patr.v2i2.48

Abstract

Fiordland is a carbon sink, and the influence of landslide events on carbon transport and sequestration in the region needs to be understood. Landslides triggered by two earthquakes in Fiordland were mapped using Google Earth Pro satellite imagery (eye altitude of 1.5–2.5 km, enabling $\pm$ 50 m precision). Ground acceleration during the 2003 M_w 7.2 Secretary Island Earthquake resulted in at least 1852 landslides. The larger 2009 M_w 7.8 Dusky Sound Earthquake had lower accelerations, producing only 313. Both events dislodged large swaths of native forest, grassland vegetation and soil, some landing in rivers and fjords. The landslide maps and magnitude–frequency distributions show close similarity to a published Global Forest Loss dataset derived from 2001–2022 satellite imagery. Assuming forest loss here is predominantly landslide related, it enables the more-precise earthquake-induced landslide mapping to be placed in a longer-term context of other vegetation loss, mostly rainfall-induced landslides, during the past two decades. The total area of forest loss during the 2003 earthquake was anomalous, whereas during 2009 the earthquake losses were similar to areas of forest loss assumed to be rainfall-induced landslides throughout Fiordland each year. Carbon concentrations of landslide vegetation were calculated by defining vegetation types from a published Land Cover Database, and soil organic carbon concentration from a 1 km resolution raster dataset. Total carbon loss from earthquake-induced landslides amounts to 2.05 Mt for the 2003 M_w7.2 and 0.217 Mt for the 2009 M_w 7.8. By way of comparison, New Zealand's total annual carbon sequestration was 6.3 Mt in 2020, and CO_2 emissions were 9.2 MtC. Multiple-occurrence regional landslide events can account for changes carbon storage and sequestration in areas of dense vegetation, such as Fiordland. Processes of landscape disturbance are significant for carbon accounting and could be included in estimates of national greenhouse gas emissions.

Introduction

Climate change and the increasing concentration of greenhouse gases in our atmosphere have driven a desire for science to account for carbon and understand its transfer between various sources and sinks. Aotearoa New Zealand provides a unique opportunity to study natural rates of carbon transfer imposed by landscape evolution. Formed by and sitting astride an active plate boundary, there are large areas in Te Waipounamu the South Island where the trees, plants, and soil are preserved in untouched wilderness. Protected by national parks and world heritage areas, the forests are largely unaffected by the influence of humans. Instead, there is disturbance to the landscape and stored carbon because of rainfall and earthquakes. The uplifting landmass intersects a westerly atmospheric circulation to produce orographic rainfall that becomes locally intense during extreme events and results in rainfall-induced landslides. On a longer time scales, the plate boundary is one of the fastest moving on the planet and results in regular strong shaking and earthquake-induced landslides. During these events, the mountainous landscape sheds carbon in the forests and soil into the rivers, lakes, and fjords. Carbon can be oxidised back into the atmosphere, consumed by ocean organisms as dissolved organic carbon (DOC) and returned to the ocean and atmosphere by respiration as CO_2, or sequestered into submarine sediment deposits.

The spectacular mountainous topography of Fiordland owes its origin to both active tectonics and past glaciation. It sits in a high rainfall area above and astride a major active plate boundary, where strong shaking can be generated from the Alpine Fault, the subduction plate interface, or several other nearby intra-plate faults. Landslides and rockfall are inevitable in the event of an earthquake, given the steepness of topography, and some of these will fall into the fjords.

The Alpine Fault traverses offshore at the western end of Milford Sound where locally it has some of the highest strike-slip rates measured on earth (Barnes, 2009; Howarth et al., 2018). The large number and regularity of past earthquakes on fault demonstrates the next event is inevitable, while the time since the last event provides statistical probability that the next earthquake is much higher than the long-term average. It is estimated that a M_w 8 or greater earthquake has a 75% chance of occurring in the next 50 years (Howarth et al., 2021).

The aim of this study was to understand the amount of carbon laterally transferred by earthquake- and rainfall-induced landslides, and its significance relative to other carbon sequestration occurring in New Zealand.

Fiordland forest change and carbon accounting.

Topography in Fiordland ranges from lowland swamps to steep mountainous terrain, and extensive U-shaped glacially eroded fjords. Fiordland is especially susceptible to landslides, due to the combination of steep topography (average slopes 35^{o} - 65^{o}) and high rainfall (ranging from ~1200 mm/y to ~6500 mm/y) (Hancox et al., 2004), and periodic strong shaking from earthquakes on the plate boundary. Earthquake-induced landslides (EIL) appear to be extremely common in Fiordland and one the largest contributors to landscape change in the region (Hancox et al., 2010). Many of the terrestrial and submarine landforms reflect these events.

Fiordland is cloaked in forest and native grass vegetation. There is much literature on the carbon budget for specific plants, specific elevations, and specific land cover types. Primarily, Tate et al. (1997) has quantified total terrestrial carbon for all vegetation types throughout New Zealand (Table 1). Soil organic carbon is as important as vegetation carbon when determining carbon loss from landslides, especially in Fiordland. Fiordland has high soil organic carbon concentrations compared to much of New Zealand (Roudier, 2022). Soil organic carbon concentration percentages are represented by a 1 km resolution raster from Roudier (2022).

Forest loss occurs annually in Fiordland (Figure 2) (Hansen et al., 2022), much because of rainfall-induced landslides. Two relatively recent earthquakes, which produced large numbers of landslides across large areas of Fiordland, also affected the amount of carbon stored on the hillslopes, or within the fjords and river systems. These were the 2003 M_w 7.2 Fiordland earthquake, and the 2009 M_w 7.8 Fiordland earthquake (Hancox et al., 2010; Hancox et al., 2004).

Table 1: Carbon reserve per unit area for landcover types in New Zealand, from Tate et al. (1997).

	vegetation class	(10^3 ha)	reserve (Mt)
C1	Orchards or vineyards & pasture	98	1.6
C2	Horticultural crops & pasture	67	0.3
	Total for Cropland	165	1.9
G1	Improved pasture	6449	19
G2	Unimproved pasture	876	1.8
G3	Short-tussock grassland	1116	12
G4	Snow-tussock grassland	1361	37
G5	Short-tussock–snow-tussock grassland	712	14
G6	Red-tussock grassland	80	1.8
	Total for Grassland	10 594	86
S1	Mixed indigenous scrub	362	36
S2	Manuka/kanuka scrub or fern	614	31
S3	Subalpine scrub	97	7.8
S4	Gorse scrub	19	1.1
	Total for Scrub	1092	76
F1	Podocarp forest	43	18
F2	Lowland podocarp–broadleaved forest	1098	371
F3	Highland podocarp–broadleaved forest	51	14
F4	Lowland podocarp–broadleaved-beech forest	1390	486
F5	Highland podocarp–broadleaved-beech forest	206	54
F6	Beech forest	2001	680
F7	Beech–broadleaved forest	114	33
F8	Broadleaved forest	223	54
F9	Exotic forest (as at 1992)	1290	125
	Total for Forest	6416	1835
M1	Subalpine or alpine herbfield	187	2.8
M2	Wetland communities	89	2.8
M3	Sand-dune communities	52	0.4
M4	Pakihi heathland communities	45	0.9
	Total for Miscellaneous	373	6.9
GS1	Grassland & mixed indigenous scrub	839	35
GS2	Grassland & manuka/kanuka scrub or fern	2229	42
GS3	Grassland & cassinia scrub	39	0.3
GS4	Tussock grassland & subalpine scrub	958	21
GS5	Grassland & *Dracophyllum* scrub	55	1.3
GS6	Grassland & gorse scrub	220	4.6
GS7	Grassland & matagouri	520	4.2
GS8	Grassland & sweet brier or sweet brier & matagouri	230	1.8
	Total for Grassland–Scrub	5090	110
GF1	Pasture & podocarp–broadleaved forest	338	35
GF2	Pasture & broadleaved forest	134	10
GF3	Pasture & beech or podocarp forest	131	14
GF4	Pasture & exotic forest	18	0.5
GF5	Tussock grassland & beech forest	100	11
GF6	Tussock grassland & podocarp–broadleaved–beech forest	10	1.6
	Total for Grassland–Forest	731	72
FS1	Kauri & manuka/kanuka or mixed indigenous scrub	50	8.6
FS2	Podocarp–broadleaved forest & scrub	447	87
FS3	Podocarp–broadleaved-beech forest & scrub	141	28
FS4	Beech forest & scrub	317	57

Approach of this study

This study uses GIS methods and statistical calculations to account for carbon during the two earthquakes, and then places these observations in a longer-term context of vegetation loss over two decades.

Landslide data

Landslides from the 2003 and 2009 earthquakes were mapped in a reconnaissance fashion immediately following the earthquakes (Hancox et al., 2004). The original set of point data for the landslide occurrences (n = 433 2003, n = 187 2009) was used as a guide for digitally mapping the landslides as polygons. Google Earth Pro (GEP) allows the user to retrospectively look at satellite imagery, including imagery from before and after the earthquakes. The landslide areas were digitally mapped using this imagery, mostly at an eye altitude of 1.5–2.5 km. All points from the original dataset were checked and re-mapped, but many more landslides were discovered that had not previously been mapped. A new inventory was constructed, which now contains 1852 landslides for the 2003 earthquake, and 313 for the 2009 earthquake. Each landslide is represented by a location point, a source area polygon, and a debris trail polygon. The magnitude and distribution of landslides (Figure 1) is a function of both topography and levels of peak ground acceleration (PGA).

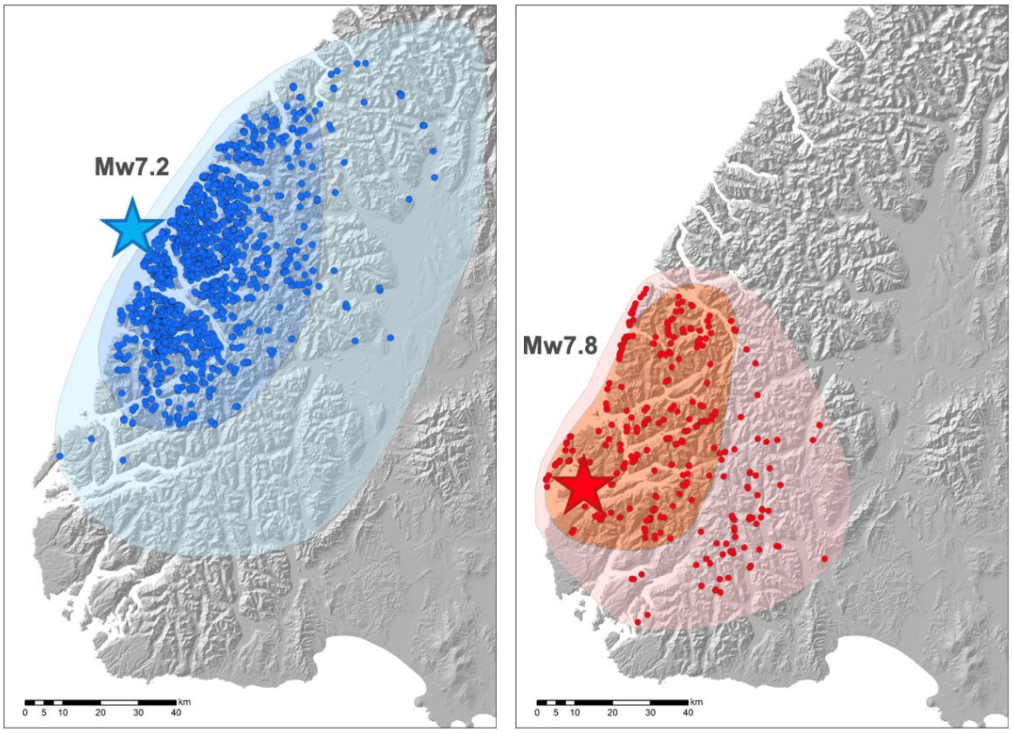

Figure 1: Landslide locations for the 2003 (left) and 2009 (right) Fiordland earthquakes. Shaded areas show concentrated areas of high landslide activity and overall extent of landslide activity. The star icons show the epicentres for each earthquake. Figure reproduced from Cox (2023).

High resolution maps of global forest change have been generated by Hansen et al. (2013); Hansen et al. (2022). These datasets show forest loss each year from 2001–2022 and forest gain during the period of 2000–2012 at 30 m resolution. Based on cumulative changes of spectral colour in satellite imagery, the dataset detects any source of forest change and in Fiordland includes both rainfall-induced and earthquake-induced landslides, as well as areas of forest clearance in valleys due to erosion. The potential of using the dataset to quantify earthquake-induced landslides generated during the 2003 earthquake was examined by Raab (2015), who found 1449 individual landslides, fewer than mapped by this study using GEP. Here we extracted data on the area of global forest change in Fiordland for the period 2001–2022 (Figure 2). The dataset shows a strong peak in 2003, which we interpret to be due to the 2003 earthquake and likely representing the large number of landslides. For the 2003 and 2009 years, when the earthquakes occurred, pixels of contiguous forest loss in the grid models were converted into polygons, from which number and areas of loss were determined for comparison with the manually mapped inventory. The total forest losses in 2003 and 2009 are plotted by area along with the mapped earthquake-induced landslide areas for 2003 and 2009 in Figures 3 and 4. There are clear similarities between the datasets in terms of total magnitude and total numbers. The number-size distribution relationships are also similar, although the forest loss dataset has characterised more smaller landslides, whereas the landslide mapping inventory has more large landslides. Based on the similarity, it seems reasonable to assume that the forest loss dataset is predominantly recording the landslide loss of vegetation from slopes. This study mapped more landslides in 2003 than 2009, and the same difference appears to be present when comparing 2003 and 2009 forest loss data (Figures 3 and 4).

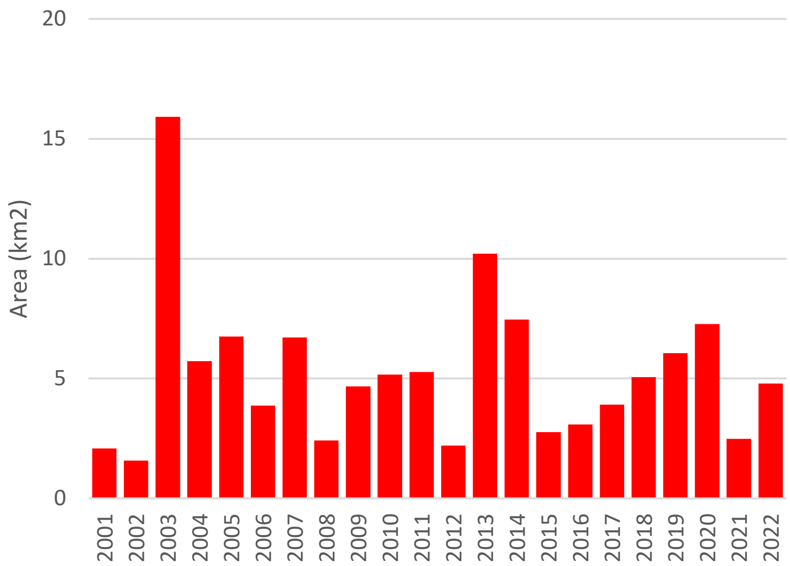

Figure 2: Area of forest loss determined from satellite imagery during the period 2001-2022, from Hansen et al. (2022).

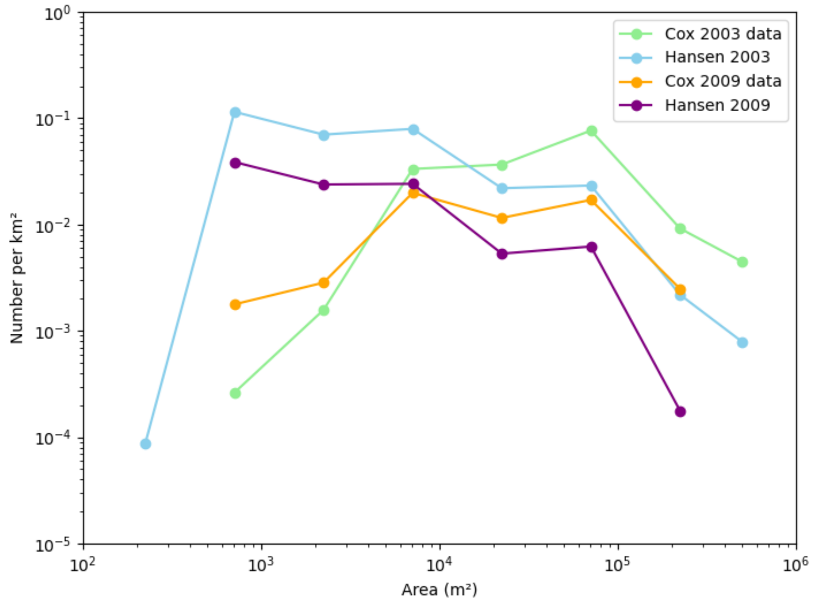

Figure 3: Normalised number size distributions of landslides mapped manually (labelled Cox 2003, Cox 2009) or from forest loss areas thought to represent landslides (labelled Hansen 2003, Hansen 2009). The size of the landslides is determined from their planimetric map area. Numbers of landslides or forest loss features were counted within a logarithmic area range bin, then divided by the land area of regional extent of landslides and plotted at the geometric mean of each bin range.

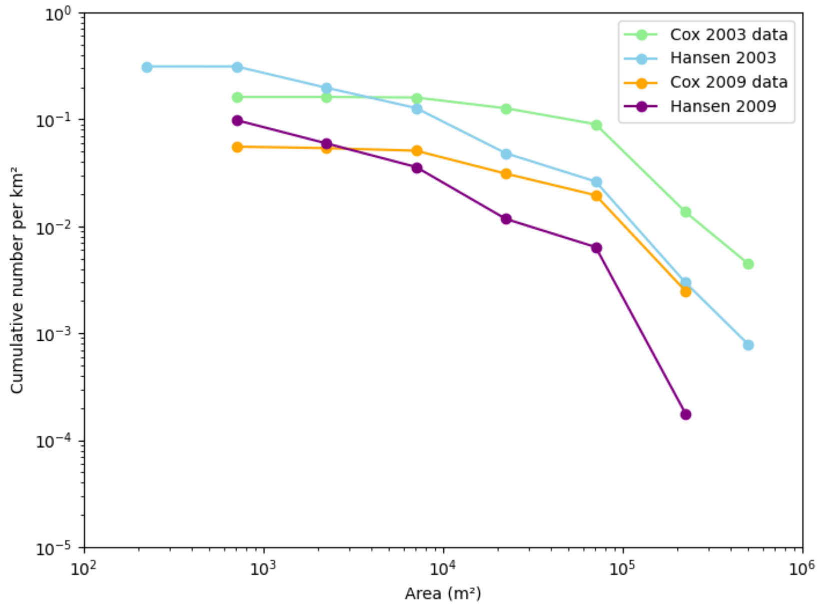

Figure 4: Cumulative normalised number size distributions for data shown in Figure 3. The number of landslides greater than or equal to a given logarithmic area range bin was divided by

the land area of regional extent of landslides, then plotted against at the geometric mean of each size range bin.

Carbon data

The New Zealand Land Cover Database (LCDB) is a multi-temporal, thematic classification of New Zealand's land cover (Landcare Research, 2019). It identifies 33 mainland cover classes. Land cover types from Tate et al. (1997) were converted to tonnes of carbon per hectare and combined with the LCDB (Landcare Research, 2019). Some data needed to be combined to better illustrate the carbon density for each type of land cover in the LCDB (Table 2). The amounts of vegetation carbon are also known to vary with elevation in New Zealand (Hall et al., 2001). Values provided by Hall et al. (2001)) and Beets et al. (2012) are comparable with values in Table 1. These vegetation data, along with soil organic carbon concentration data, were then joined to landslide polygons to develop statistics on carbon concentration for Fiordland EIL. Topographic slope model statistics were recorded from the New Zealand 8m Digital Elevation Model (LINZ, 2012), resampled to 15 m resolution, for the same polygons.

Table 2: Vegetation types recorded by the landcover database of New Zealand, and their calculated carbon densities.

Name	**Area**	**Carbon Reserve**	**Vegetative carbon (t/ha)**
Alpine Grass/Herbfield	3376	65.8	19.49
Broadleaved Indigenous Hardwoods	223	54	242.15
Indigenous Forest	5126	1710	333.59
Fernland	614	31	50.49
Flaxland	89	2.8	31.46
Manuka and/or Kanuka	614	31	50.49
Matagouri or Grey Scrub	520	4.2	8.08
Sub Alpine Shrubland	958	21	21.92
Tall Tussock Grassland	80	1.8	22.5

Results

The total amounts of carbon, including the amount of organic carbon from soil and carbon from vegetation, for both landslides, are provided in Tables 3 and 4. Over two Mt of carbon were dislodged in landslides during the 2003 M_w 7.2 earthquake dislodged, whereas only about one-fifth of that was dislodged during the 2009 M_w 7.8 earthquake. Landslide area was compared to total carbon entrained within landslides (Figure 5) and shows a similarity between the two earthquake events. Intuitively, as landslide area increases, the amount of carbon transported by the landslide increases. Amounts of vegetation and soil organic carbon transported within each landslide also have similarity (Figure 6). A significant number of the landslides either intersected rivers or landed in the fjords. Of the carbon laterally transported by the landslides, 58.9 % in 2003 (Figure 7), and 52.44 % in 2009 (Figure 8), was indirectly connected to rivers and fjord waterway, where it could be transported and potentially or stored within the fjords themselves. The rest of the carbon remained stored on slope in landslide deposits and may be subject to biodegradation.

Table 3: 2003 M_w 7.2 Fiordland earthquake soil, vegetation, and total carbon amounts (tonnes) transported by landslides.

Soil organic carbon 2003	**Vegetation carbon 2003**	**Total carbon 2003**
$1x10^6$	$1.05x10^6$	$2.05x10^6$

Table 4: 2009 M_w 7.8 Fiordland earthquake soil, vegetation, and total carbon amounts (tonnes) transported by landslides.

Soil organic carbon 2009	**Vegetation carbon 2009**	**Total carbon 2009**
$1.14x10^5$	$1.03x10^5$	$2.17x10^5$

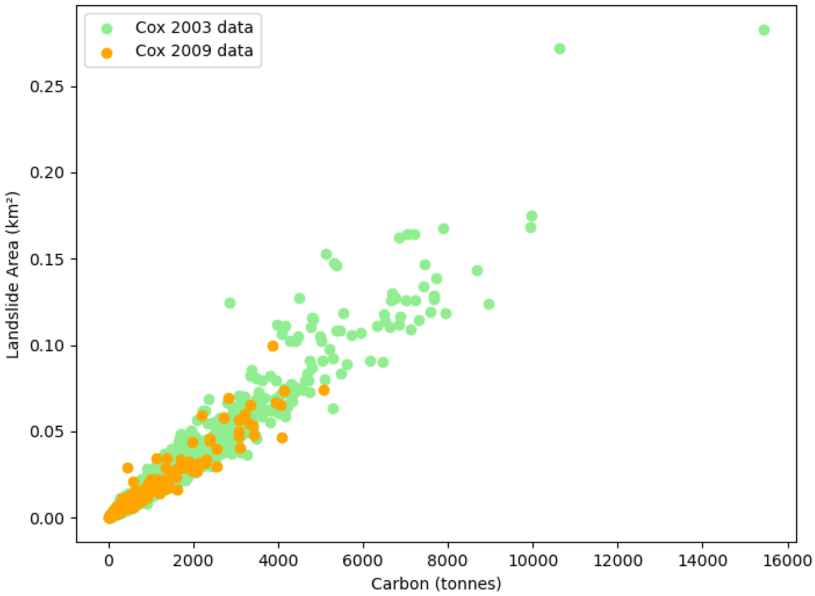

Figure 5: Landslide area is compared to carbon loss (tonnes) for the 2003 and 2009 Fiordland earthquakes. Each dot represents a landslide from the mapped inventory.

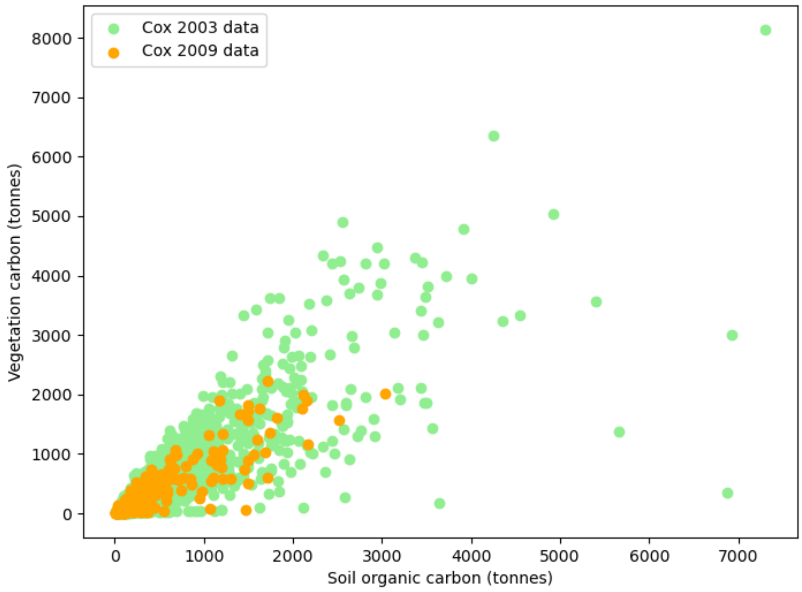

Figure 6: Vegetation carbon loss (tonnes) is plotted against soil organic carbon loss (tonnes) for the 2003 and 2009 Fiordland earthquakes. Each dot represents a landslide from the mapped inventory.

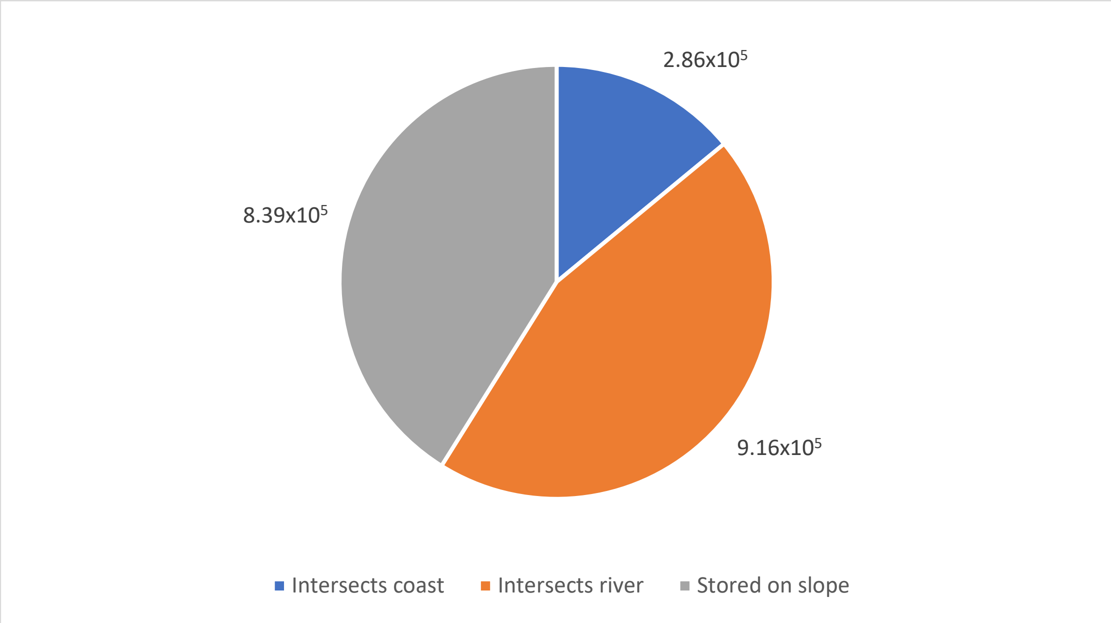

Figure 7: Carbon storage on slope (in tonnes) compared to areas where landslides intersect rivers and the coast for the 2003 M_w 7.2 Fiordland earthquake.

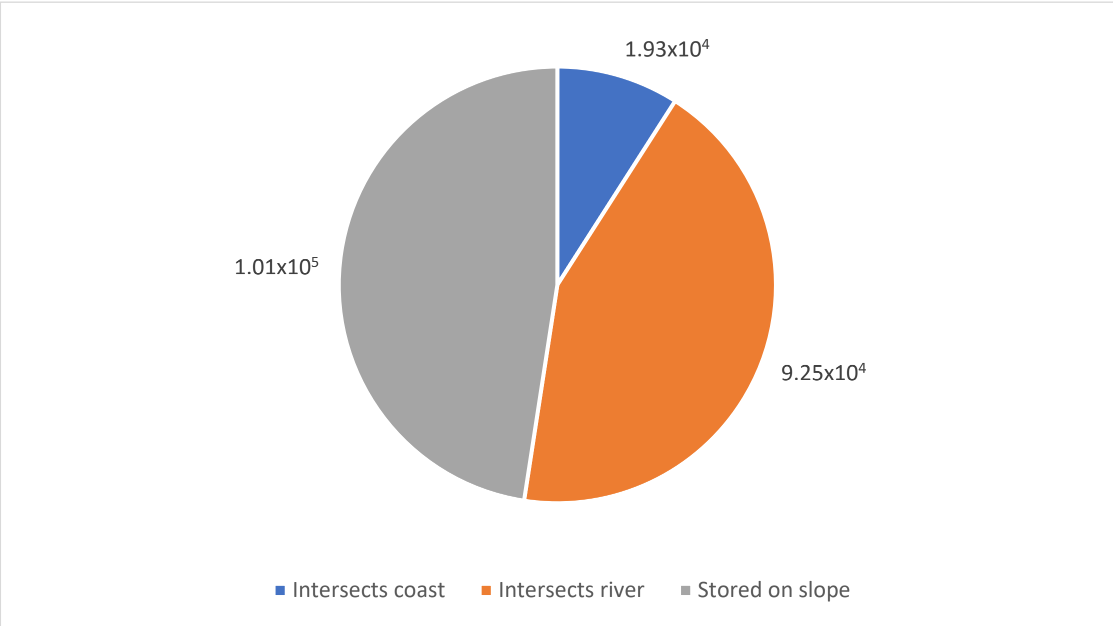

Figure 8: Carbon storage on slope (in tonnes) compared to areas where landslides intersect rivers and the coast for the 2009 M_w 7.8 Fiordland earthquake.

Indigenous forest is by far the largest singular vegetation type both within the landslides and within wider representative extents of landslides that affected Fiordland during the earthquakes (Figures 9-12). Tall tussock grassland is an equally significant proportion of the wider representative areas of 2003 and 2009 landslides (being ~17-18%), but less so (~5-7%) of areas that failed as landslides. This is likely due to the topography where these tall tussocks grow, which is less steep and less prone to landsliding. All other vegetation types cover much less area in Fiordland but are still significant contributors to the totals in Tables 3 and 4. Other land cover types include lakes, gravel and rock, landslide scars and introduced pastoral land, among others. These were less significant contributors to the overall soil and vegetation carbon budget, therefore were not included in this study.

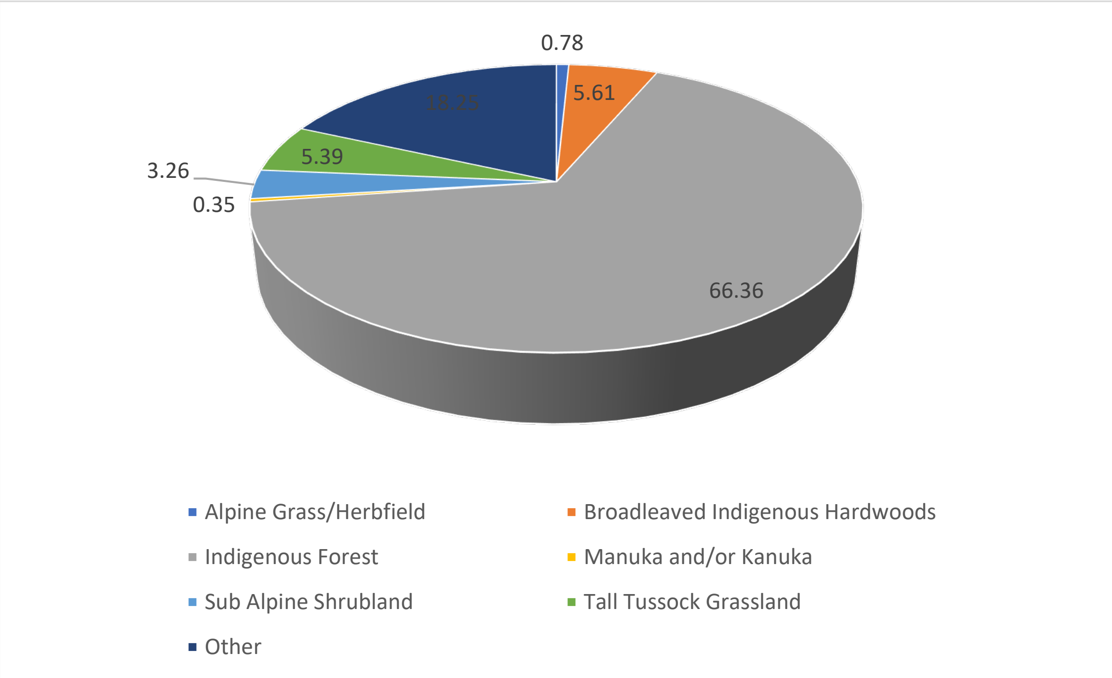

Figure 9: Vegetation types as a percentage of area of landslides generated during the 2003 M_w 7.2 Fiordland earthquake.

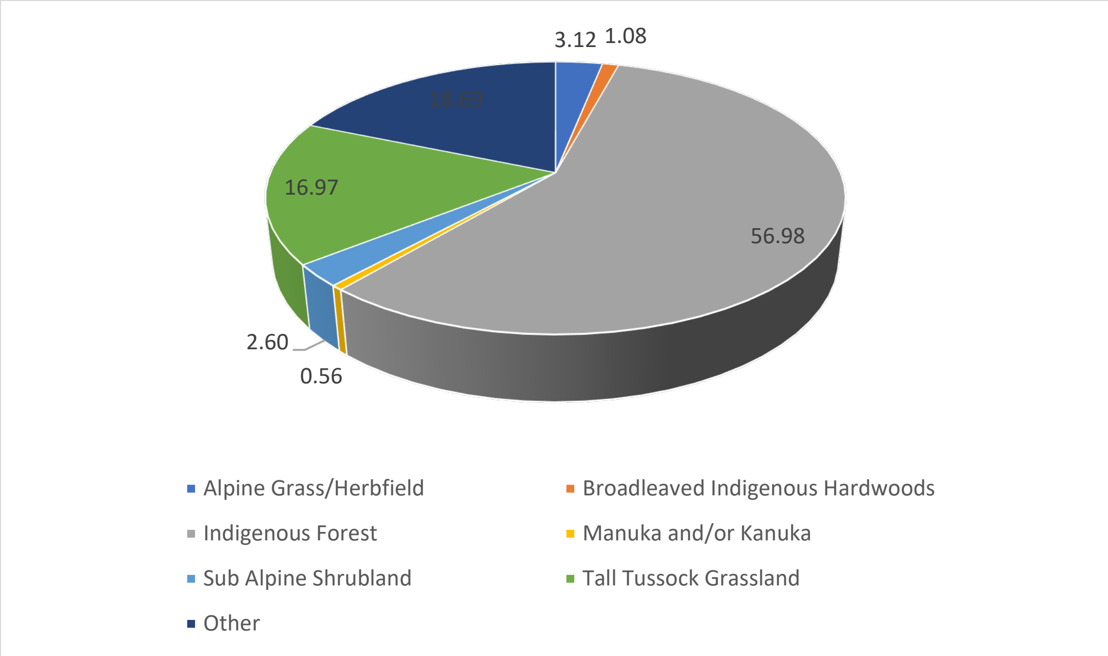

Figure 10: Vegetation types as a percentage of a wider representative area of Fiordland defined by the total extent of landslides during the 2003 M_w 7.2 Fiordland earthquake (see Figure 1).

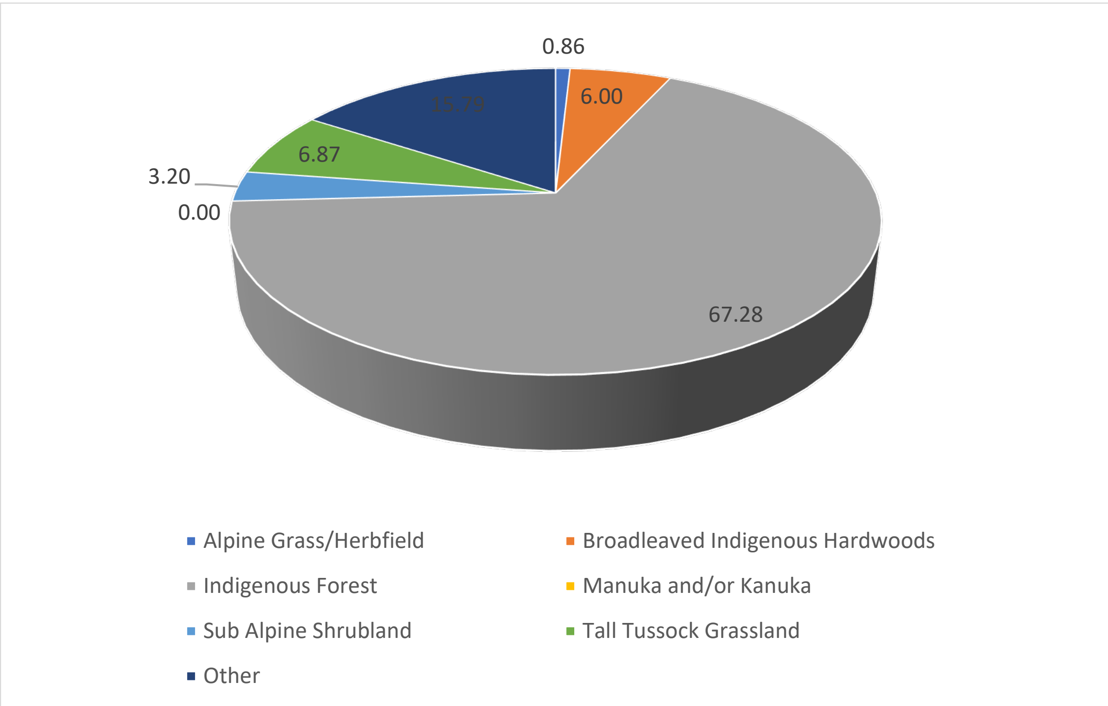

Figure 11: Vegetation types as a percentage of area of landslides generated during the 2009 M_w 7.8 Fiordland earthquake.

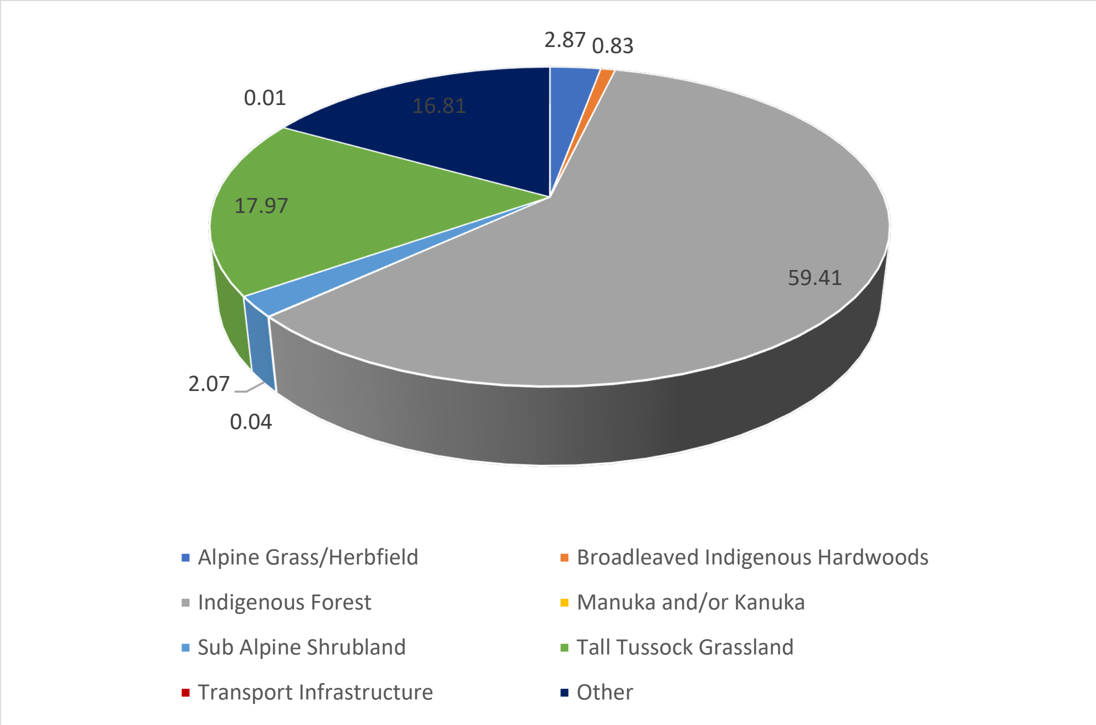

Figure 12: Vegetation types as a percentage of a wider representative area of Fiordland defined by the total extent of landslides during the 2009 M_w 7.8 Fiordland earthquake.

Discussion

Although the 2003 Fiordland earthquake had an extremely high landslide count, these can be considered in context of wider forest loss over time using data from Hansen et al. (2022) (Figure 2). During the two decades from 2001-2022, it appears the inter-earthquake annual forest losses in the absence of earthquakes (which is assumed to be mostly rainfall-induced landslides) total as many, if not more, than losses due to earthquake events. The loss of forest in 2009, which seems likely due to the M_w 7.8 earthquake, is similar in scale to that of other non-earthquake years. The magnitude of landslide activity from singular earthquakes (Figure 1), along with the topography and geology of the Fiordland region, suggest that all of Fiordland has potential to have experienced at least one landslide in the past. This could explain why vegetation in Fiordland is so young (Johnson, 1976). The removal of soil due to landslides may expose rock and inhibit rejuvenation of forest cover (Stewart, 1986).

Over 2 Mt of carbon was either biodegrading or being stored within the fjord systems due to the 2003 and 2009 Fiordland earthquakes (Tables 3 and 4, Figures 7 and 8). This compares with a similar order of magnitude of carbon (4.5 ± 0.8 Mt) thought to have been sequestered by New Zealand's plantation forests between 1 April 1988 and 1 April 1989 (Hollinger et al., 1993). With landslides having such a major influence on carbon transport and potential sequestration in Fiordland, whether they be either rainfall- or earthquake-induced, it is clear they should probably be considered when accounting for New Zealand's total carbon budget. In 2020, New Zealand's total sequestered carbon was 6.3 Mt (Berg, 2008; Stats New Zealand, 2024). New Zealand's emissions calculations count any loss of forest to be a loss of carbon (Ministry for the Environment, 2023). New Zealand's total CO_2 emissions were 9.2 MtC in 2020 (Ministry for the Environment, 2023), and total emissions of all gases were 22 MtC when converted from CO_2e (80 $MtCO_2e$). The next challenge regarding understanding Fiordland is to develop ways to measure the proportion of carbon displaced by landslides that ends up sequestered within the fjords, compared with that which is oxidised on slopes or at sea. Understanding the relative proportions of particulate organic carbon (POC) and dissolved organic carbon (DOC) (Scott et al., 2006), and whether these differ in streams draining landslide areas from elsewhere in Fiordland, is a fertile area for future work.

A source of uncertainty for this study comes from the steepness of topography and GIS-based calculations based on area in 2D plan-view. Higher resolution and more accurate digital elevation models (DEM's) for the Fiordland region would undoubtedly improve calculations. As slopes are very steep, the use of planimetric area and generalised models could also be improved in the future by using 3D models and mapping landslides in 3-dimensions. The mapped landslide polygons from GEP are limited by the capture date of available satellite imagery. Some landslides which were assumed to be earthquake-induced may potentially be older or younger than the earthquake, and may potentially be rainfall-induced. However, a strong correlation between visible landslides and previously mapped points, as well as the distinctness of large landslides near other EIL, suggest this is only a minor issue in these data. The values used for carbon concentration in the vegetation were also estimated from vegetation types (Tate et al., 1997), then checked with concentrations as per elevation, and might be improved with more granular definition of local vegetation and actual data on carbon from Fiordland. The Hansen et al. (2022) dataset also only maps vegetation loss from the year of most apparent change, therefore, may miss data where there has been loss in multiple years, especially if there is a difference in the scale of loss between years.

Concluding remarks

The 2003 M_w 7.2 and 2009 M_w 7.8 Fiordland earthquakes caused 2.2 Mt of carbon from vegetation and soil to mobilise and distribute throughout the fjords, rivers, and slopes. That is in contrast with the approximately 4.5 ± 0.8 Mt of carbon sequestered by New Zealand's plantation forests between 1 April 1988 and 1 April 1989 (Hollinger et al., 1993). The 2003 and 2009 earthquakes also only contributed to 18% of the landslide activity recorded by Hansen et al. (2022) in Fiordland during the period from 2001–2022. It appears the natural rate of loss of stored carbon from Fiordland due to active landscape processes, averaged between rainfall-induced and earthquake-induced landslides over two decades, is likely to be a significant 0.1–1 Mt per year. To put into context, New Zealanders would need to plant 550,000 hectares of radiata pine trees to replace this carbon, based on Berg (2008). Mapping and analyses of the data in this study would be greatly improved by higher spatial resolution and more accurate elevation and vegetation data. Higher temporal and spatial resolution satellite imagery would aid development of future landslide datasets. Investigation of carbon transport is valuable for carbon sequestration and climate related research, especially in areas such as Fiordland. Natural landscape change processes appear to be significant in the context of carbon accounting, so should probably be included in estimates of national carbon budgets. The next challenge in Fiordland is to understand the proportion of landslide-related carbon that becomes transported as dissolved organic carbon (DOC) versus particulate organic carbon (POC), and account for amounts sequestered within reducing environments deep in the fjords, versus that released to the atmosphere by oxidation on mountain slopes and/or carried offshore and oxidised in the Tasman Sea.

Acknowledgements

This project was funded by the Centre for Sustainability, University of Otago, through a summer research scholarship. Primary supervision was given by Caroline Orchiston, and I am very grateful for the time and effort she put into my project. I would like to thank Pierre Roudier, Simon Cox and Chris Massey for their guidance and assistance with data regarding this project. I would also like to extend my gratitude to Jocelyn Turnbull and Pascal Sirguey for their advice and knowledge. And to Chris Moy, Christina Riesselman, Andrew Gorman, Bob Dagg, and the rest of the Polaris II crew, thank you for the opportunity to be involved with the November 2023 Fiordland research cruise. The opportunity to see the area first-hand was invaluable. This manuscript has been improved through by comments and suggestions of two anonymous referees.

References

Barnes, P. M. (2009). Postglacial (after 20 ka) dextral slip rate of the offshore Alpine fault, New Zealand. *Geology*, *37*(1), 3-6.

Beets, P. N., Kimberley, M. O., Oliver, G. R., Pearce, S. H., Graham, J. D., & Brandon, A. (2012). Allometric Equations for Estimating Carbon Stocks in Natural Forest in New Zealand. *Forests*, *3*(3), 818-839. https://www.mdpi.com/1999-4907/3/3/818

Berg, P. (2008). *Radiata pine - Multi-purpose plantations*. Te Ara - the Encyclopedia of New Zealand. http://www.TeAra.govt.nz/en/radiata-pine/page-5

Cox, S. C. (2023). Earthquakes and landslides in Fiordland. FACET IDCP Workshop, Dunedin.

Hall, G. M., Wiser, S. K., Allen, R. B., Beets, P. N., & Goulding, C. J. (2001). Strategies to estimate national forest carbon stocks from inventory data: the 1990 New Zealand baseline. *Global Change Biology*, *7*(4), 389-403.

Hancox, G., Cox, S., & Jongens, R. (2010). *The nature and significance of landslides caused by the Mw 7.6 earthquake of 15 July 2009 in Fiordland, New Zealand*.

Hancox, G., Cox, S., Turnbull, I., & Crozier, M. (2004). Landslides and other ground damage caused by the MW7. 2 Fiordland earthquake of 22 August 2003. Proceedings of the 9th Australia New Zealand Conference on Geomechanics,

Hansen, M., Potapoc, P., Moore, R., & Hancher, M. (2022). *Global Forest Change*. https://glad.earthengine.app/view/global-forest-change#bl=off;old=off;dl=1;lon=20;lat=10;zoom=3;

Hansen, M. C., Potapov, P. V., Moore, R., Hancher, M., Turubanova, S. A., Tyukavina, A., Thau, D., Stehman, S. V., Goetz, S. J., & Loveland, T. R. (2013). High-resolution global maps of 21st-century forest cover change. *science*, *342*(6160), 850-853.

Hollinger, D., Maclaren, J., Beets, P., & Turland, J. (1993). Carbon sequestration by New Zealand's plantation forests. *New Zealand journal of forestry science*, *23*(2), 194-208.

Howarth, J. D., Barth, N. C., Fitzsimons, S. J., Richards-Dinger, K., Clark, K. J., Biasi, G. P., Cochran, U. A., Langridge, R. M., Berryman, K. R., & Sutherland, R. (2021). Spatiotemporal clustering of great earthquakes on a transform fault controlled by geometry. *Nature Geoscience*, *14*(5), 314-320.

Howarth, J. D., Cochran, U. A., Langridge, R. M., Clark, K., Fitzsimons, S. J., Berryman, K., Villamor, P., & Strong, D. T. (2018). Past large earthquakes on the Alpine Fault: paleoseismological progress and future directions. *New Zealand Journal of Geology and Geophysics*, *61*(3), 309-328.

Johnson, P. (1976). Vegetation associated with kakapo (Strigops habroptilus gray) in Sinbad gully, Fiordland, New Zealand. *New Zealand Journal of Botany*, *14*(2), 151-159.

Landcare Research. (2019). *LCDB v5.0 - Land Cover Database version 5.0, Mainland, New Zealand* (https://lris.scinfo.org.nz/layer/104400-lcdb-v50-land-cover-database-version-50-mainland-new-zealand/

LINZ. (2012). *NZ 8m Digital Elevation Model* (https://data.linz.govt.nz/layer/51768-nz-8m-digital-elevation-model-2012/

Ministry for the Environment. (2023). *Te ine tukunga: He tohutohu pakihi. Measuring emmsions: A guide for organisations*. Te Kāwanatanga o Aotearoa - New Zealand Government

Raab, T. (2015). *Geomorphological Indicators of Slope Instabilities in Alpine Settings* TECHNISCHE UNIVERSITÄT MÜNCHEN].

Roudier, P. (2022). *Soil, Aotearoas most precious resource - past, present and future.* Blenheim.

Scott, D. T., Baisden, W. T., Davies-Colley, R., Gomez, B., Hicks, D. M., Page, M. J., Preston, N. J., Trustrum, N. A., Tate, K. R., & Woods, R. A. (2006). Localized erosion affects national carbon budget. *Geophysical Research Letters*, *33*(1).

Stats New Zealand. (2024). *New Zealand's greenhouse gas emissions*. https://www.stats.govt.nz/indicators/new-zealands-greenhouse-gas-emissions

Stewart, G. H. (1986). Forest dynamics and disturbance in a beech/hardwood forest, Fiordland, New Zealand. *Vegetatio*, *68*, 115-126.

Tate, K., Giltrap, D., Claydon, J., Newsome, P., Atkinson, I., Taylor, M., & Lee, R. (1997). Organic carbon stocks in New Zealand's terrestrial ecosystems. *Journal of the Royal Society of New Zealand*, *27*(3), 315-335.